FABRICATION AND OPTIMIZATION OF CARBON FIBER MICROELECTRODES FOR IN VIVO DETECTION OF ACETYLCHOLINE IN RAT HIPPOCAMPI

FABRICATION AND OPTIMIZATION OF CARBON FIBER MICROELECTRODES FOR *IN VIVO* DETECTION OF ACETYLCHOLINE IN RAT HIPPOCAMPI

A thesis presented by Anna M. Sellon

to the Faculty of the College of Arts and Sciences

of the University of Vermont

In Partial Fulfillment of the Requirements

of the University of Vermont Honors College

and Bachelor of Science in Neuroscience

May 2023

Defense Date: 24 April 2023

Thesis Examination Committee:

Yangguang Ou, Ph.D., Advisor

Allison Anacker, Ph.D., Chairperson

Jeremy Barry, Ph.D.

Abstract

Abnormal release of acetylcholine (ACh) in the brain has been implicated in major neurological disorders like epilepsy, however little technology has been developed to allow for real-time, rapid, and spatially precise *in vivo* measurements of this neurotransmitter. We optimized carbon fiber microelectrodes (CFMs) for such measurements using surface adsorption of acetylcholinesterase (AChE) and choline oxidase (ChO) followed by electrochemical deposition of Nafion. Sensitivity, stability, and selectivity were characterized via flow injection analysis and *in vivo* measurements were taken in rat hippocampi, all using fast-scan cyclic voltammetry (FSCV). We established a 1:10 ratio of AChE:ChO to be the most optimal with a highly linear calibration curve (r^2=0.986) as well as a limit of detection of 0.814 mM and a limit of quantification of 2.711 mM. The electrodes demonstrated high selectivity against dopamine and ascorbic acid ($p<0.0001$) and remained stable throughout multiple injections over the course of several hours (r^2=0.053). Significant *in vivo* events were recorded and quantified. These results suggest that FSCV on CFMs hold promise for continuous and spatiotemporally sensitive measurements of ACh *in vivo*. Further optimization and *in vivo* testing may broaden the applications of this ACh CFM for eventual use in elucidating the treatment of other ACh-related diseases like Parkinson’s and Alzheimer’s.

Introduction

Epilepsy is a debilitating disorder that affects over 3 million people in the United States alone.[1] Focal seizures, specifically in the temporal lobe, are the most prevalent form of epilepsy. Over time, these can lead to significant deficits in episodic memory,[2] a type of long-term memory consisting of lived experiences. These deficits make it a great priority for the medical community to better understand the neural and chemical correlates of the disorder as well as to develop preventative measures against such effects. One current focus is on the role of disrupted neural oscillations, specifically theta oscillations (4-12Hz), in the contribution to this memory loss. Lesion studies have demonstrated the critical role of theta oscillations in normal hippocampal function[3], making them essential for the formation and retrieval of learning and memory. During an epileptic seizure in the temporal lobe, there are significant decreases in theta oscillation power and frequency as well as delayed synchronization between hippocampal regions, as reviewed by Shuman et al.[4] Abnormal theta oscillations are therefore implicated in the cognitive disruption associated with epileptic seizures. Understanding the molecular underpinnings of these theta disruptions is necessary for understanding epilepsy-associated memory loss. ACh is a prime candidate for the molecular mechanism underlying this pathology because one of the major inputs to the hippocampus that has been associated with theta oscillation generation, the medial septum-diagonal band of Broca (MS/DB), has a high density of cholinergic neurons.[5] Indeed, studies have shown theta oscillations to be induced by cholinergic agonists[6] and suppressed by cholinergic antagonists.[7] This makes the precise interplay between ACh release and theta oscillations a promising avenue for gaining critical insight into the nature of theta oscillations and how they are disrupted in pathological conditions. However, the specific contributions of these cholinergic neurons to theta oscillations as well as how they innervate the hippocampus are still highly debated.[5] For example, there are two subtypes of theta oscillations, with type 1 theta (6-12 Hz) being associated with movement and type 2 theta (4-9 Hz) occurring during immobility. Historically, it was though that only type 2 theta was sensitivity to cholinergic perturbation.[8] However, Gu and Yakel[9] have recently shown that type 1 theta is also sensitive to cholinergic disruption, as discussed in their review. Such controversies are exacerbated by a currently lack of technology available that allows for continuous, rapid, and spatially precise measurements of ACh fluctuations *in vivo*.

Microdialysis is the most prominent quantitative technique used in the field today to measure ACh levels and is considered the gold standard for continuous chemical monitoring. However, it requires 10-20 minutes[10] for each sample collection, which is much longer than each neurotransmission event. This makes it difficult to correlate sample collected with specific neurotransmission events. Additionally, microdialysis probes range from 0.2-0.6 mm in outer diameter,[11] which prevents measurements specific to brain regions in rodents with brain sizes on the scale of millimeters. The relatively large size of these probes presents another issue of tissue damage, which may provoke an immune response and potentially reduce measurement accuracy.[12]

One promising, relatively unexplored technique for taking *in vivo* measurements is electrochemical monitoring, in which the oxidation and reduction peaks of electroactive molecules are used to measure their concentration in the environment.[10] Zhang et al.[13] demonstrated the effectivity of amperometry, one method for such electrochemical monitoring, in bridging this gap by detecting choline concentration in rat hippocampi as in indicator for ACh concentrations. They found a significant association between theta oscillations and ACh release. However, this study was limited in that the sensors used, ceramic-based multielectrode arrays, had a time resolution of

2 seconds, a size on the scale of hundreds of microns, and its measurements were dependent on the natural breakdown of ACh.[13]

Fast scan cyclic voltammetry (FSCV) at carbon fiber microelectrodes (CFMs) is a promising alternative due to the small size of the electrode (less than 10 microns in diameter) and the ability of the technique to take rapid measurements at a timescale of 100 milliseconds.[10] Due to their smaller size, CFMs also result in less damage to tissue upon insertion than microdialysis and ceramic-based multielectrode arrays.[10] Further, the activated carbon surfaces of CFMs increase electrode biocompatibility and provide a versatile platform that can be adapted for different analytes.[10] Keighron et al.[14] demonstrated the potential for carbon-fiber based ACh electrodes *in vitro*, both in a flow cell and model cell, to have significant sensitivity and selectivity for fluctuating ACh concentrations. Limitations of this study were that their probes were relatively large at 30 microns in diameter and that they also used amperometry, a technique that can take real-time measurements but has a relatively low signal output that makes it difficult to record low concentrations (i.e. poor sensitivity). Navera et al.[15] developed and characterized a Nafion-coated CFM selective for ACh, however their probes were approximately 200 μm in diameter and they used slow-scan cyclic voltammetry, which limits temporal resolution to tens of seconds with a frequency of less than 0.1 Hz. Since we are interested in measuring ACh concentration changes on the same time scale as that of theta oscillations (4-12 Hz), we require a technique capable of making more rapid measurements. Thus, there is still a need for a small, functional CFM probe that can amplify signal for recording rapid, potentially small fluctuations of ACh concentrations *in vivo*.

FSCV on CFMs is a promising technique for bridging this gap. FSCV is a background subtracted technique in which only changes in current can be measured, making it well-suited for determining fluctuations in analyte concentrations. A schematic overview of FSCV can be found in Figure 1, reproduced from Ou et al.[16] With an application frequency of 10 Hz, FSCV can be used to take rapid measurements on the scale of 100ms, allowing for detection of transient chemical events on comparable timescales as theta oscillations. Additionally, the standard waveform applied to the electrode, originally established for dopamine detection, can be modified for enhanced selectivity of a specific analyte (Figure 1a-b). Further, most analytes have a unique voltage at which they are oxidized or reduced, enabling the identification of a specific molecule when multiple electroactive analytes are present (Figure 1d). FSCV at CFMs also allow for measurements from different spatial scales. For example, a 100 micron long cylindrical CFM (7 micron in diameter) allows for chemical measurements from a few hundred synapses,[17] indicating its high spatial sensitivity. Combined with the fact that it can be used for continuous monitoring, this technique holds promise for the ACh detection we seek.

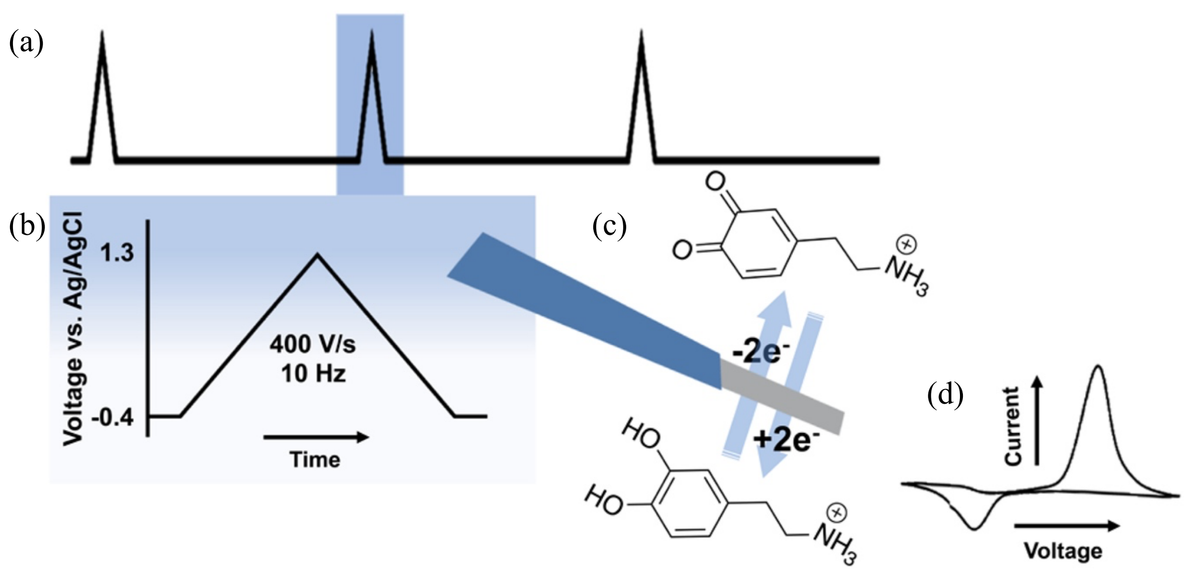

Figure 1. Schematic of FSCV applied to a CFM, reproduced from Ou et al.[16] (a) The established DA waveform and (b) the waveform parameters that can be modified for other molecules of interest. (c) The oxidation and reduction of DA that occurs at the surface of the CFM when the waveform is applied. (d) The resulting cyclic voltammogram output, with the current from the oxidation being the upper peak and that from the reduction being the lower peak.

As implied above, electroactivity, or the ability to be oxidized and reduced, in the analyte of interest is required for FSCV and for all other electrochemical methods. Previous literature states that ACh is non-electroactive,[15] further verified by my own experiments (Figure 3a). To circumvent this issue, as established in several other prior studies,[14,15,18] we took a dual enzyme approach in which acetylcholinesterase (AChE) and choline oxidase (ChO) are co-immobilized onto the surface of the electrodes. Together, the enzymes break ACh down into hydrogen peroxide (H_2O_2) though the following reactions:

$$Acetylcholine \xrightarrow{AChE} Choline + Acetate$$

$$Choline + O_2 \xrightarrow{ChO} H_2O_2 + Betaine$$

Hydrogen peroxide is a highly electroactive molecule for which CFMs have been developed in the past,[19] making it a promising proxy for ACh.

The purpose of this research is to optimize the ratio of AChE:ChO on CFMs for consistent and reliable ACh detection, with the goal of taking rapid and spatially precise *in vivo* recordings of ACh fluctuations in the rat hippocampus.

Methods

Chemicals

AChE from electrophorus electricus (>1000 U/mg), ChO (>10 U/mg) from Alcaligenes, and ascorbic acid were bought from Sigma-Aldrich (St. Louis, MO). Acetylcholine chloride was bought from Thermo Scientific. Nafion (1000 EW at 15% weight) was purchased from Ion Power (New Castle, DE). Bovine serum albumin (BSA) was gifted by Dr. James Stafford's lab (Department of Neurological Science, University of Vermont). Phosphate buffered saline was made from tablets purchased from Fisher BioReagents. Sodium phosphate dibasic and sodium phosphate monobasic were purchased from Fisher Chemical. Hydrogen peroxide and ethanol were purchased from Fisher Scientific, and dopamine was purchased from Alfa Aesar.

Electrode Fabrication

Carbon fiber microelectrodes were prepared by aspirating a single 7 μm diameter carbon fiber strand through a borosilicate glass capillary tube (1.0 mm x 0.5 mm, 4", A-M Systems, Sequim, WA) before being tapered by a commercial pipette puller (models PE-22 and PC-100, Narishige Japan). Exposed carbon fiber was cut to 100 ± 10 μm in length with a scalpel and a nichrome wire (Weico Wire & Cable Inc., Long Island, NY) coated in silver paint (Silver Print II, GC electronics) was inserted into the capillary tube to electrically connect the carbon fiber wire.

Electrode Pretreatment

The following electrode modification procedure was adapted from Navera et al.[15] Electrodes were washed in ethanol followed by water before being oven-dried for 5 min at 70-75 °C. The sensors were then pretreated using chronoamperometry at 1.2V versus pseudo Ag/AgCl in PBS, applied by a WaveDriver 100 EIS Potentiostat (Pine Research, Durham, NC). Pretreatment results in the addition of oxygen-containing groups to the carbon surface of the electrode, which provides the oxygen needed for the conversion of choline to hydrogen peroxide by ChO.

Enzyme Solution Preparation

Enzyme solutions were prepared using specific ratios of AChE:ChO either based on unit of enzyme activity[15] (1 U/mg/mL) or by mass,[14] indicated throughout the paper. All ratios included 2 mg/mL BSA for enzyme immobilization. Solutions were either prepared with PBS or 50 mM sodium phosphate buffer (pH = 7.4). If not used immediately, solutions were stored at -20 °C and thawed when ready for use. Following pretreatment, electrodes were placed in 1 mL aliquots of the enzyme solutions for 16-18hrs, allowing for passive adsorption to the carbon fiber surface.

Nafion Coating

Following overnight enzyme preparation, electrodes were removed from the enzyme solutions and dried at room temperature for 15 minutes. Nafion was then electrochemically deposited onto the surface of the carbon fiber following the protocol of Hashemi et al.[20] Briefly, each electrode was lowered into the Nafion solution via a micromanipulator for 30 seconds with a constant potential of 1.0V versus pseudo Ag/AgCl applied to the electrode. Electrodes were then dried at room temperature for another 15 minutes before use. Nafion is needed to keep the enzymes adhered to the carbon fiber surface. Additionally, it is a cation-exchange polymer, meaning that it helps prevent the mass transfer of anions to the surface of the electrode and, by extension, help prevent the collection of signals from other molecules like ascorbic acid commonly found in the brain.

Flow Injection Analysis (FIA) and Data Collection

All optimization was conducted using a custom FIA set up. Each CFM was screwed into the flow cell in which the reference pseudo Ag/AgCl electrode was also housed. A syringe pump (Fisherbrand model 100, Fisher Scientific) was used to continuously flow PBS past the electrodes at a rate of 1.81 mL/min, and a six-port injection valve was used to introduce the analyte in 5 second boluses.

Custom WCCV 3.6 software (Knowmad Technologies LLC, Tuscon, AZ) was used for all data collection and analysis. As we are oxidizing H_2O_2 as a proxy for ACh, we used the standard H_2O_2 waveform[19] of -0.4 to 1.4V at a scan rate of 400 mV/S and a frequency of 10 Hz for all experiments. Text files of cyclic voltammograms and current versus time graphs (IT curves) were exported from the WCCV 3.6 software at 1.3V (2410 point number) and processed in both Excel (Version 16.71) and GraphPad Prism 9. Current density was calculated by averaging the currents of the plateau in each IT curve and dividing that by each electrode surface area. A trial was considered unsuccessful if no plateau was observed. An unpaired t-test and simple linear regression were performed for statistical analyses and outliers were assessed via Grubbs' test.

In Vivo Measurements

All *in vivo* measurements were made with the help of Dr. Jeremy Barry. A 4 month old male rat was anesthetized with 1.6-1.7 mg/kg urethane in sterile saline, bought from Sigma Aldrich, via intraperitoneal injection.[21] In one hemisphere, a 64-channel laminar silicone probe with 20 µm between each electrode (purchased from Cambridge NeuroTech) was placed in the hippocampus through craniotomy and stereotaxic surgery.[21] The CFM was implanted into the contralateral hemisphere. Figure 2b, modified from Kloc et al.,[22] demonstrates the approach of our probes in the rat hippocampus. Simultaneous measurements were taken at 3.59, 3.62, 3.68, 3.75 mm depths, verified by histology.

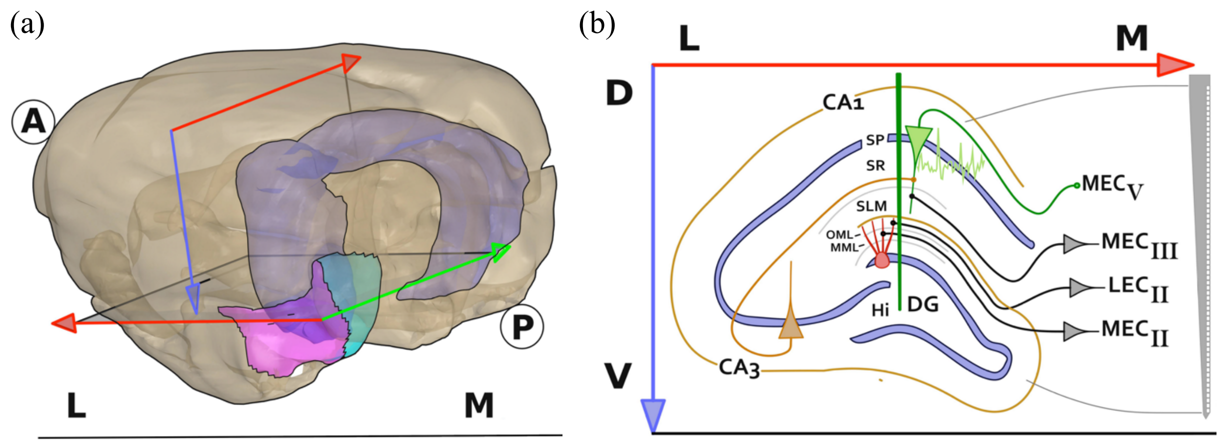

Figure 2. Diagram of the rat brain and hippocampus, modified from Kloc et al.[22] L and M represent Lateral and Medial directions, A and P indicate Anterior and Posterior directions, and D and V represent Dorsal and Ventral directions. (a) Location of the dorsal and ventral hippocampus (purple) in the coronal (red-blue arrows) and horizontal (red-green arrows) planes. The medial and lateral entorhinal cortex (MEC and LEC) is also pictured in blue and pink respectively. (b) Placement of the CFM, represented by the green line, in the rat hippocampus. Some inputs to the hippocampus are also pictured, with L3 MEC projecting to CA1 as well as L2 LEC and MEC projecting to the outer and middle molecular layer (OML and MML respectively) of the dentate gyrus (DG). Both the MEC and LEC generate theta oscillations of different frequencies.

Results and Discussion

Acetylcholine and Hydrogen Peroxide Oxidation

As mentioned previously, electroactivity of the analyte is necessary to employ FSCV. To verify that ACh does not have this property, we injected 1mM ACh through a flow injection analysis (FIA) system past the surface of the electrode while applying a default waveform. No current was detected (Figure 3a), confirming its lack of electroactivity as well as the need to modify the carbon fiber surface for ACh detection. Our lab has demonstrated, through work spearheaded by Nathan Robins, that our electrodes are linearly sensitive to increasing concentrations of hydrogen peroxide (r^2=0.98), as seen in Figure 3b and c. The modification of our CFM surface with AChE and ChO for H_2O_2 detection as a proxy for ACh concentration should therefore be effective.

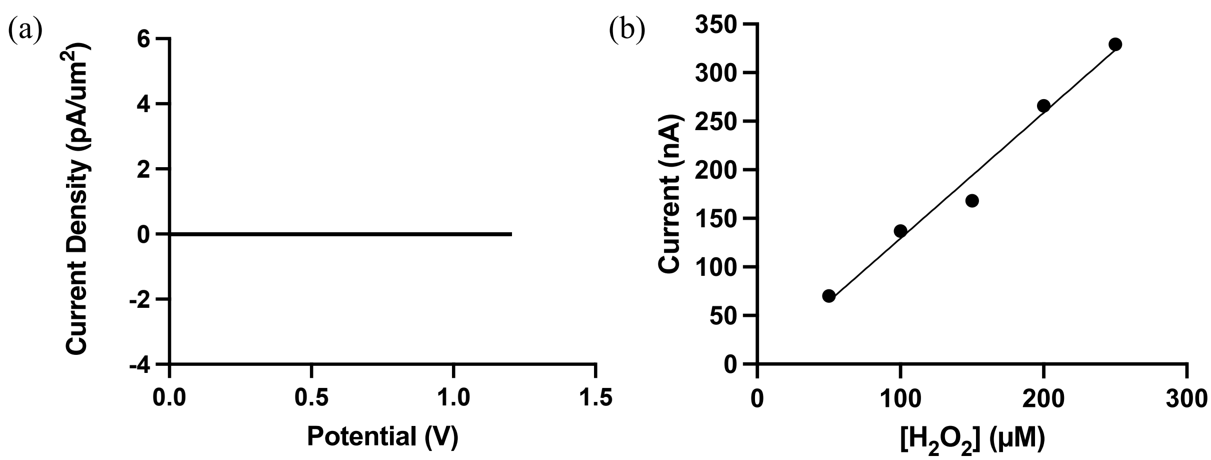

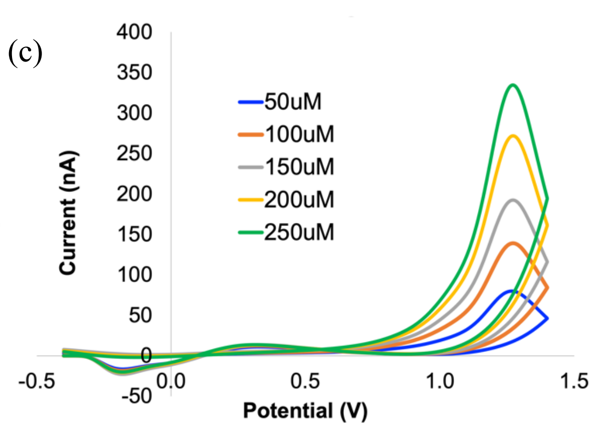

Figure 3. (a) Cyclic voltammograms taken after ACh injection with a bare CFM (n=3 electrodes). (b) Calibration curve of current output (R^2=0.98, n = 1 electrode) and (c) cyclic voltammograms taken with a bare CFMs after 50µm to 250µm H_2O_2 injections.

Enzyme Ratio Optimization

In order to maximize sensitivity and consistency of the CFMs, various ratios of AChE:ChO were tested for their efficacy in producing current from H_2O_2 oxidation proportional to the injected ACh concentrations. There are two primary ways to calculate enzyme ratio: by unit of enzymatic activity and by mass. Following the protocol of Navera et al.,[15] we initially made all ratios in terms of enzymatic activity. As ChO is much less active than AChE at 10 U/mg compared to 1000 U/mg, we tested ratios with significantly higher concentrations of ChO than AChE to maximize H_2O_2 output. However, a further search of the literature revealed that ratios by mass may be more reliable. Keighron et al.[18] found that the ratio of AChE and ChO adhered to the surface of their electrodes was significantly different from that of the solution. X-ray crystallography established that the shape of AChE tends to be spherical[23] while ChO[24] is cylindrical, potentially accounting for the difference in affinity for the electrode surface[18] and thus the altered ratio. Additionally, Keighron et al.[18] found that the specific activity of AChE decreased from 1000 U/mg to 125 $\pm$ 18 U/mg after binding to the electrode surface while that of ChO remained approximately the same. Although this data was collected for enzyme adsorption onto gold nanoparticles,[18] their findings hold important implications for carbon fiber. Theoretically, decreased enzymatic activity can be expected after binding to any surface due to potential alterations in protein conformation and subsequently altered active site configurations. Alternatively, the active site of any given enzyme may be blocked by the electrode itself after adsorption, decreasing the functional activity of the enzymes. Calculating the ratio based on units of enzymatic activity is therefore not a reliable method, as such activity will likely be different for each electrode despite being placed in the same initial ratio. Calculating the ratio by mass, however, is more reliable because it remains more constant even in the face of activity change, assuming the enzymes are independent from each other. Before proceeding with the ratios calculated by mass, we did a direct comparison between the two methods, seen in Figure 4. We wanted to compare and contrast the calibration curves for 1:1.8 AChE:ChO by unit activity vs. 1:1.8 AChE:ChO by mass because the latter uses significantly fewer amount of enzymes, especially for ChO, making it more cost effective. We wanted to verify that the signals from both would be comparable if we did switch to mass ratio system. Simple linear regression revealed that ratios by both mass and by unit had a high level of correlation between ACh concentration injected and the current density recorded (r^2=0.80 and r^2=0.93 respectively). While the higher r^2 value for the by unit ratio suggests a better linear fit, in practice both are equally variable and have a small (and rather high) range for linear dynamic range, which makes the sensors not sensitive enough for use *in vivo*. The 50 mM and 70 mM ACh injections for the ratio by unit did not have a significantly different current output (p=0.42) and the 70 mM ACh injection for the ratio by mass was much higher than the 90mM injection (Figure 4). As making the ratios by mass is also more cost effective because it uses less enzymes and Figure 4 indicates there is no loss in sensitivity compared to making sensors using unit ratios, we proceeded with testing ratios by mass and converted all ratios by unit into their by mass equivalent.

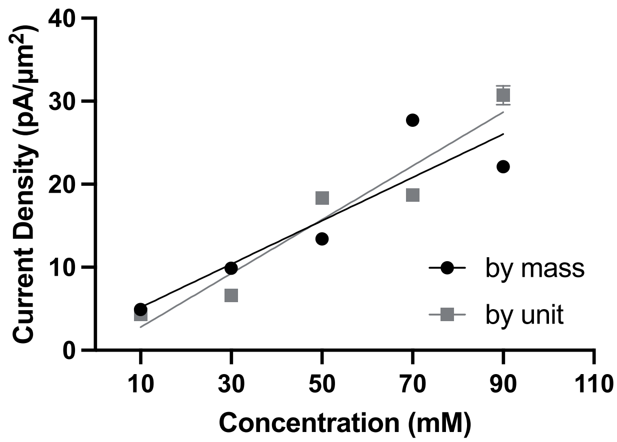

Figure 4. Calibration curve comparison between ratio of 1:1.8 AChE:ChO calculated by mass (r^2=0.80) versus by unit of enzymatic activity (r^2=0.93). Error bars are ±1 SEM, n=4 electrodes.

A full list of all ratios tested can be found in Table 1. We began by testing a ratio of 1:18.7 AChE:ChO by mass, adapted from the enzymatic ratio established by Navera et al.,[15] at various

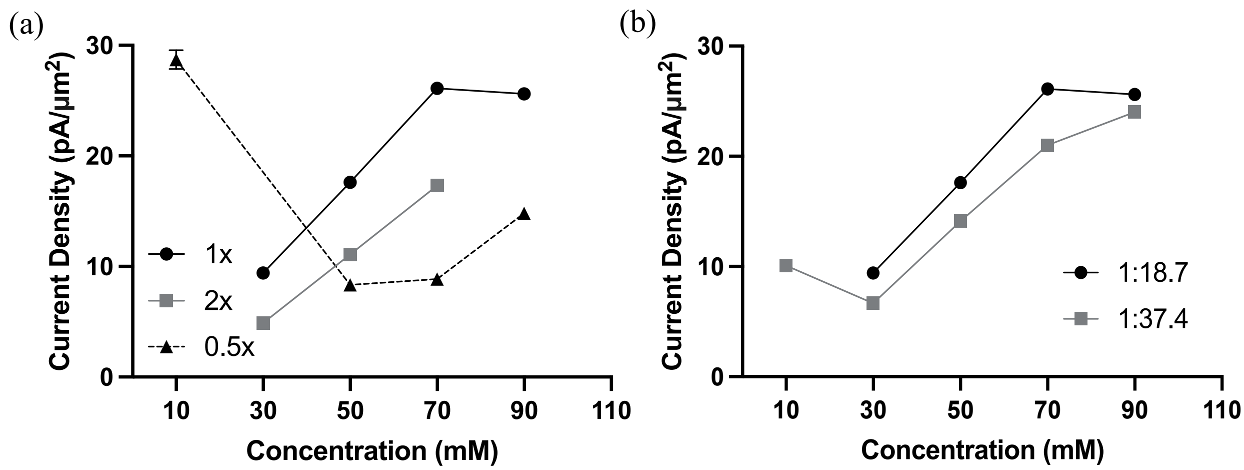

Figure 5. Calibration curves for non-optimal ratios comparing (a) the same 1:18.7 AChE:ChO ratio by mass at 1x, 2x, and 0.5x the standard[15] enzyme concentration and (b) two different ratios by mass at 1x enzyme concentration. 10, 30, 50, 70, and 90 mM ACh were injected via FIA for all conditions. Any missing data points convey the inability for the electrodes to detect the associated concentration. Error bars are $\pm$1 SEM, n=3-5 electrodes per condition.

enzyme concentrations (Figure 5a). A significant decrease in current was observed with CFMs prepared in solutions with doubled enzyme concentrations compared to the 1x solution ($p<0.0001$). We hypothesize this is due to enzyme oversaturation, in which the close vicinity and high concentration of enzymes may have led to aggregation, altered conformation due to enzymatic interactions, and a subsequent decrease in available active sites. 0.5x concentration also largely exhibited decreased current compared to the 1x solution (Figure 5a), possibly due a lack of enzyme availability and a subsequent lack of full enzymatic coverage of the carbon fiber surface. The exception is the 10 mM ACh concentration that demonstrates the variability and inconsistency of this ratio and enzyme concentration. Taken together, the standard 1x concentration yields the highest current and is thus the concentration we carried forward in the following ratios.

The non-optimal ratios were consistently limited by similar issues, the most prominent being plateaus in the calibration curve. Exemplified by the 1:18.7 AChE:ChO ratio, current output typically remained the same at concentrations of 70 mM ACh and above (Figure 5b). This is likely the point of enzyme saturation, above which the given ratio cannot process all of the ACh available.

A similar detection limit was frequently hit at concentrations of 30 mM ACh and below, as seen in the 1:37.4 AChE:ChO ratio (Figure 5b); 10 mM ACh was highly variable in whether the CFMs register a current change, with 1:18.7 not being able to detect it at all (Figure 5b). Despite the consistently linear relationship between ACh concentration and current output for 30-70mM ACh, these enzymatic ratios were therefore not sensitive enough for reliable *in vivo* use; a given current recorded could not be attributed to a specific ACh concentration.

Of the ratios tested (Table 1), we determined 1:10 AChE:ChO by mass to be optimal. There is a strong positive correlation between ACh concentration injection and current output (r^2=0.986) when a linear regression model is applied to the 1:10 calibration curve (Figure 6a), also reflected in the cyclic voltammograms and current versus time plots (Figure 6b-c). This linearity is promising for *in vivo* use of the electrodes, since any current recorded that falls within the range

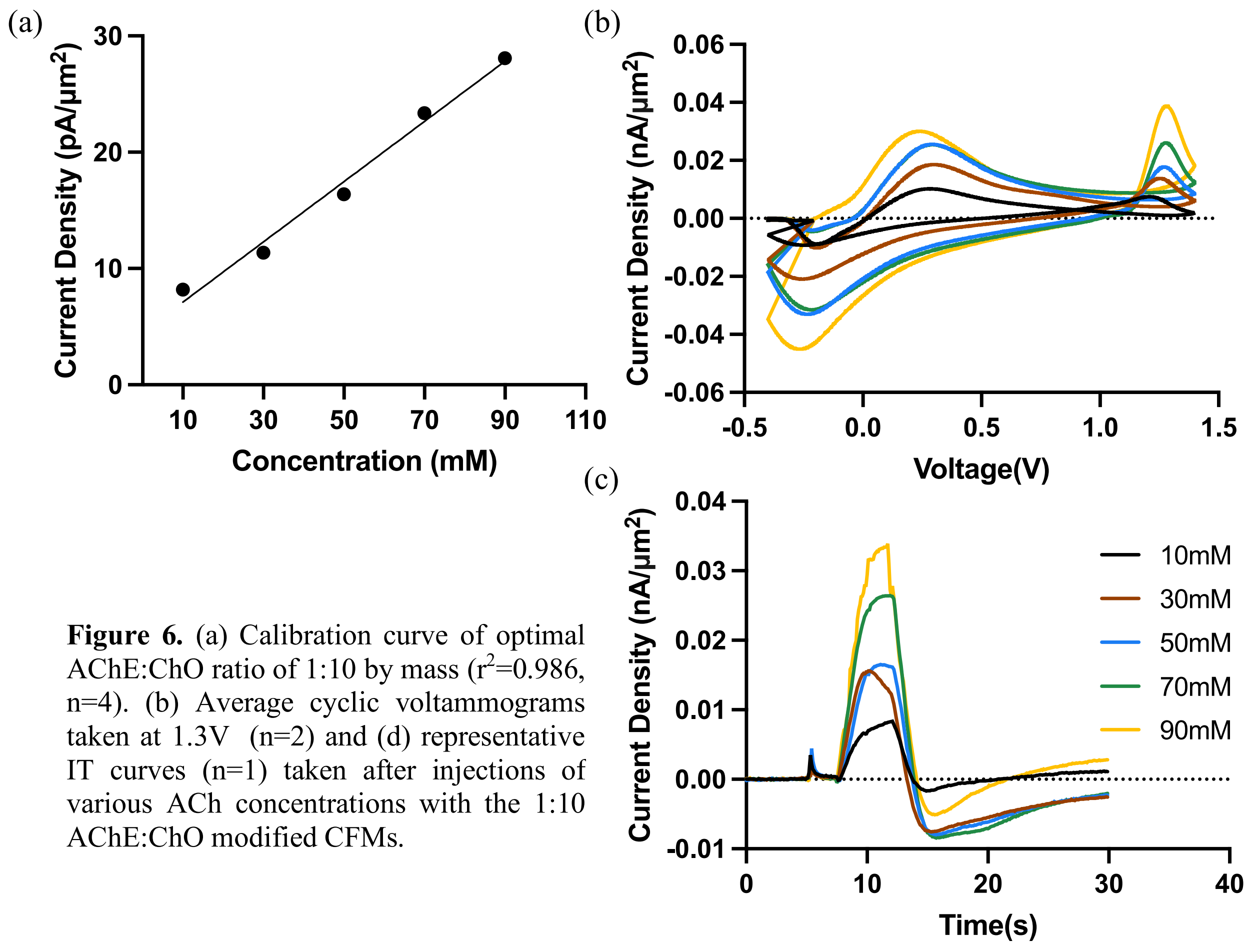

Figure 6. (a) Calibration curve of optimal AChE:ChO ratio of 1:10 by mass (r^2=0.986, n=4). (b) Average cyclic voltammograms taken at 1.3V (n=2) and (d) representative IT curves (n=1) taken after injections of various ACh concentrations with the 1:10 AChE:ChO modified CFMs.

of this plot can be attributed to a specific and singular ACh concentration. Additionally, this enzyme ratio yielded the most consistently successful electrodes. As mentioned previously, a trial was considered unsuccessful if no plateau was observed in the current versus time curve. For previous ratios, as mentioned earlier, there was high variability in whether a given electrode could successfully measure all tested ACh concentrations. The success rate for all ratios can be found in Table 1. This lack of reproducibility between electrodes was concerning, as there is no way to test

Table 1: Success rate for the detection of each ACh concentration injected via FIA, separated by the AChE:ChO ratio used to modify the CFM. Success was defined by the presence of a plateau in the current versus time curve.

			ACh Concentration (mM)					
Ratio	[Enzymes]	n	1	10	30	50	70	90
1:18.7	1x	5	0.375	0	0.429	0.833	1	1
1:18.7	2x	3	0	0	0.667	1	1	-
1:18.7	0.5x	3	-	0.25	0	1	1	1
1:37.4	1x	3	-	0	0.667	1	1	0.667
1:74.8	1x	4	-	0	0.5	1	1	1
1:1.8	1x	5	-	0.8	0.8	1	0.6	1
1:10	1x	4	-	1	1	1	1	1

for whether an electrode can measure the full range of ACh concentrations before *in vivo* use unless first tested with a calibration curve *in vitro*, something that would be time intensive and further limit the total possible amount of recording time *in vivo* before potential electrode fouling. The electrodes modified by the 1:10 ratio, however, were entirely reproducible. Of the four tested, all were able to measure each ACh concentration reliably and with consistent current output (Table 1). These results are corroborated by previous findings of 1:10 as the optimal ratio for CFMs coated in gold nanoparticles.[18]

Sensor Characterization

To understand sensitivity, selectivity, and stability of the optimal ratio, the modified CFMs were further tested via FIA. The theoretical limit of detection (LOD) and limit of quantification (LOQ) for the 1:10 ratio were first calculated using the standard deviation of background noise in n=5 randomly selected IT files as well as the linear regression equation of the calibration curve (Figure 6a). This methodology, as well as the calculated LOD and LOQ (Table 2), is in sharp contrast to the non-optimal ratios, in which we considered the empirical LOD and LOQ to be reached when the calibration curve plateaued. Since these are empirical LOD/LOQ, we currently do not have any uncertainty to report for them. The 1:10 ratio had over a ten-fold decrease in LOD and LOQ compared to the 1:34.7 ratio (Table 2), included as an example non-optimal ratio, further validating that 1:10 is the most optimal ratio tested.

Table 2: The limit of detection (LOD) and limit of quantification (LOQ) for the optimal 1:10 ratio and a sample non-optimal ratio of 1:34.7

Ratio	LOD (mM)	LOQ (mM)
1:10	0.814 ± 0.0008	2.711 ± 0.0026
1:34.7	9	30

The sensitivity of the 1:10 ratio shows promise for *in vivo* recordings of ACh release. Microdialysis studies have estimated that basal levels of ACh in the extracellular space exist in the high nanomolar to low micromolar range.[25,26] Although available technology is not yet capable of measuring concentration of ACh release on a synaptic level, a model made by Aidoo & Ward[27] suggests that the initial concentration is approximately 300 mM. As our probes record ACh release from hundreds of synapses, diffusion of the neurotransmitter combined with the magnitude of synapses recorded suggest we can expect ACh concentrations in the high micromolar to low millimolar range. The 1:10 modified CFMs therefore have a high enough maximum detection limit, though whether the probes are sensitive to smaller ACh events is less certain.

Selectivity of the 1:10 AChE:ChO modified CFMs was next characterized through the testing of potential interferents found *in vivo* via FIA. H_2O_2 was tested due to the inability of our electrodes to differentiate between the molecule and ACh, ascorbic acid was tested since it is highly abundant in the brain, and DA was tested as an industry standard. All species had significantly lower current output than the lowest tested concentration of 10 mM ACh in our calibration curve ($p<0.0001$; Figure 7b). DA was barely detectable at 1.3V, indicating that it does not readily interfere with the ACh signal and is thus not a large concern for *in vivo* electrode use (Figure 7b). Ascorbic acid (AA) also had a low current output, though it is within our LOD and therefore may be high enough to interfere with the ACh signal. As ascorbic acid is widely found

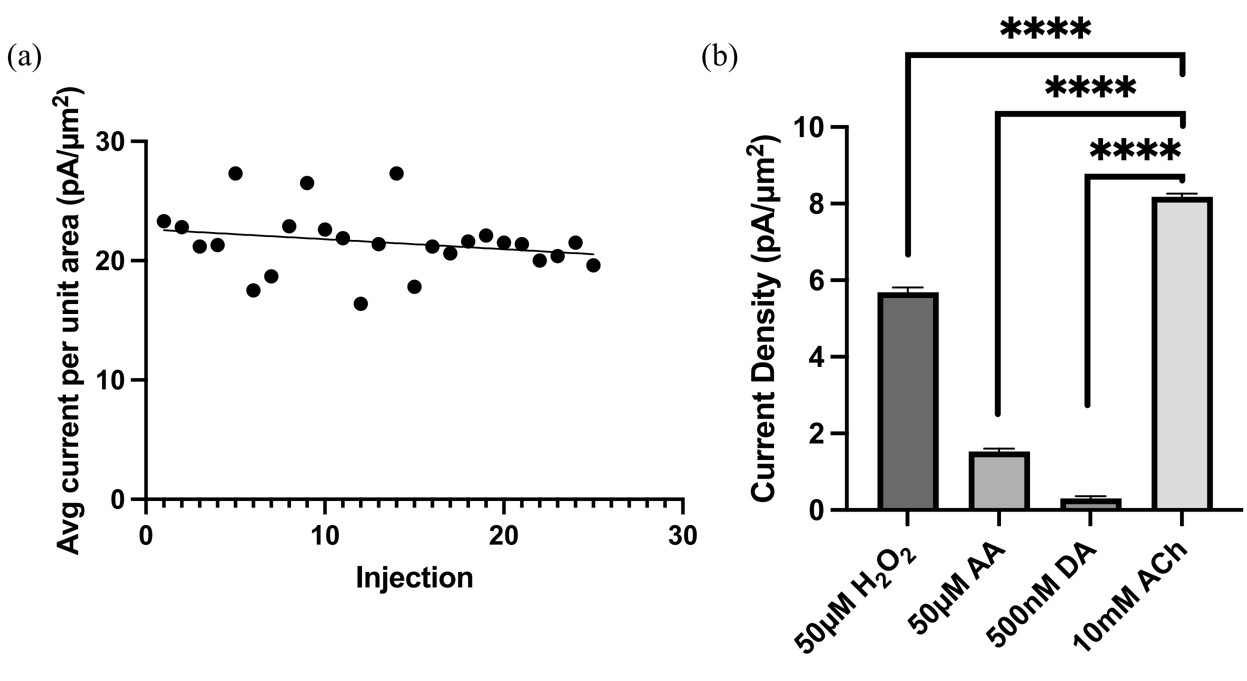

Figure 7. (a) Characterizing the stability of current output over the course of n=25 70 mM ACh injections using the 1:18.7 enzyme ratio, with 5 min of cycling between each injection ($r^2=0.053$, n=2 electrodes). (b) Testing of 50 µM H_2O_2, 50 µM ascorbic acid (AA), and 500 nM dopamine (DA) as potential interferents (n=3 electrodes per condition). All data files were taken at 1.3V where ACh oxidation is normally observed, even if other oxidations were present at different voltages. Error bars are ±1 SEM.
****$p<0.0001$

throughout the brain, this could be a potential concern. However, any basal levels of ascorbic acid will be background subtracted through FSCV and will not interfere with current output. Additionally, increasing the thickness of Nafion via a longer period of electrodeposition will likely further decrease the signal and limit its potential as an interferent, a step we will next optimize. Although significantly smaller than 10 mM ACh, H_2O_2 produced a relatively large current response (Figure 7b). Since our bare CFMs are highly sensitive to H_2O_2, this was expected. However, the concentration tested was much higher than the concentration of free H_2O_2 in the brain. Upper limits have been estimated to range from 100 nM to 1 μM levels in rodent brains,[28] suggesting that any functional H_2O_2 our electrodes encounter in the brain will produce a much smaller current output than seen in Figure 6b and potentially have minimal interference with the ACh signal. We plan to replicate this interference testing with 1 μM H_2O_2 to verify this hypothesis.

Stability of the enzymes on the CFMs was assessed through a series of n=25 injections of 70 mM ACh that took place over the course of several hours, mimicking the timescale needed for most *in vivo* experimental procedures. Although this was done with the 1:18.7 ratio and only n=2 electrodes, the current remained relatively consistent over the course of the experiment and did not significantly deviate from the initial injections ($p=0.269$, $r^2=0.053$; Figure 7a). This suggests that the enzymes on our electrode are stable and are not extremely sensitive to the changing voltage applied, allowing for continuous monitoring applications *in vivo*. Though there visually seems to be a wider variability in current response for 7 of the middle injections (Figure 7a), these are not significant outliers and this may be due to the use of the non-optimal ratio. We will therefore repeat this experiment with electrodes modified with the 1:10 ratio.

Preliminary in Vivo Experiments

In collaboration of Dr. Jeremy Barry, we tested one of our electrodes in a urethane anesthetized rat by taking 60 second recordings at various depths in the hippocampus following a tail pinch. Sensory stimulation via tail pinch under urethane is an established method for inducing theta oscillations coupled with increased ACh release,[8,13,29-36] and is therefore a reliable method for testing whether our electrodes can detect ACh fluctuations *in vivo*. We were able to record

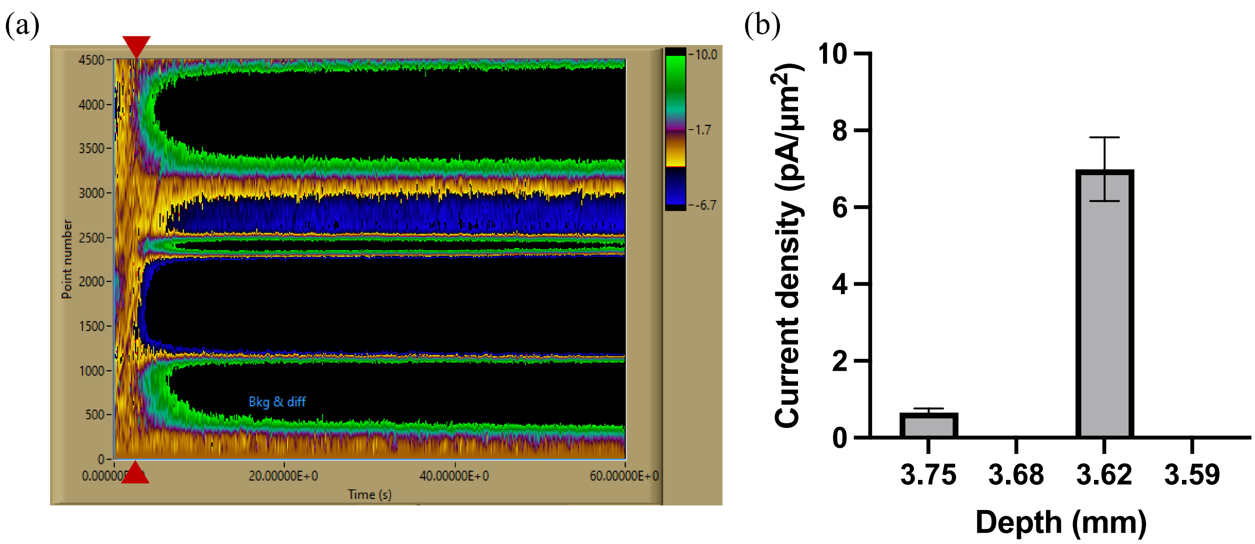

Figure 8. (a) Color plot of a significant *in vivo* event following a tail pinch at a time point indicated by the red triangles, recorded at 4.62 mm in a rat hippocampus with a 1:18.7 AChE:ChO modified CFM. The color scale represents current in nA. (b) Average amplitude of ACh-like events at varying depths in the rat hippocampus, taken from the same set of experiments as shown in (a). Error bars are $\pm$1 SD, n=1 electrode.

significant ACh-like events, as seen by the middle green smear in the color plot taken at approximately 3.62 mm (Figure 8a). Figure 8b quantifies the current density output, with the average of the color plot event represented by the bar at 3.62 mm. This depth aligns with the location of the dentate gyrus in the hippocampus, the subregion that is thought to receive the highest density of cholinergic projections from the medial septum.[37,38] It therefore makes sense that the greatest signal recorded was in that region. We were also able to record a smaller event at 3.75 mm (Figure 8b), demonstrating that our electrodes are spatially sensitive. Figure 9, reproduced from Dannenberg's dissertation,[39] shows the spatial distribution of cholinergic neurons in the rat hippocampus, with the scale also verifying our spatial sensitivity; as there are density differences in cholinergic projections between different subregions of the hippocampus that are greater than the length of our carbon fiber (approximately 100 microns), it is highly likely that we hit actual depth differences during our recordings. Considering this experiment was conducted using the non-optimal 1:18.7 AChE:ChO ratio, there is great promise for what our optimal 1:10 modified electrodes may be able to detect. We plan to test these 1:10 AChE:ChO sensors *in vivo* in the near future.

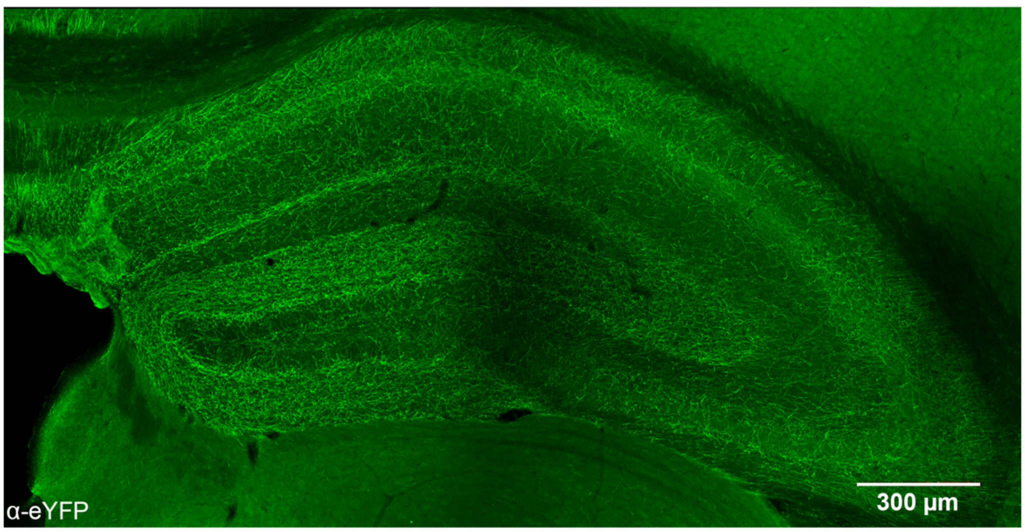

Figure 9. Reproduced from Holger Dannenberg's dissertation.[39] Confocal image of 50 μm coronal slice showing cholinergic fibers projecting from the medial septum to the hippocampus of a mouse brain. See original paper for immunohistochemical staining details. Scale bar of 300 microns included for reference.

Frequency Limitation

It is necessary to include that our application frequency of 10 Hz sets limitations on what can be reliably analyzed. According to Nyquist frequency rules, only half of the frequency applied by instrumentation can be reliably measured. This means that with FSCV at 10 Hz we can only record theta oscillations of a low, 4-5 Hz frequency. It is therefore imperative to be aware of the possibility of aliasing when analyzing signal output. While this is a large limitation, there is no current technique available that has improved performance.

Hygroscopicity of ACh

Although not directly tied to the efficacy of the electrodes, it is worth noting the highly hygroscopic nature of ACh and the importance of careful handling. As hygroscopicity means that ACh readily absorbs water from the air, improper storage conditions and handling can lead to accumulating water in the stock sample; when making solutions, if not careful, the massed amount of ACh will likely hold a significant quantity of water, making the ultimate solution less concentrated than calculated. The inconsistency in these measurements may lead to inconsistent current outputs and an inaccurate calibration curve that may skew any *in vivo* data interpretation as well. The hygroscopicity of ACh is not mentioned in most studies using the molecule. We were therefore unaware of this for the first several months of testing. To see if exposure to air made a significant impact on current output, we compared the data collected before and after realizing this potential issue. For the after condition, a new bottle of ACh was purchased and stored in a desiccator, only brought out for brief periods of time before being quickly returned. While massing the ACh in an anerobic glove box would have been ideal, we

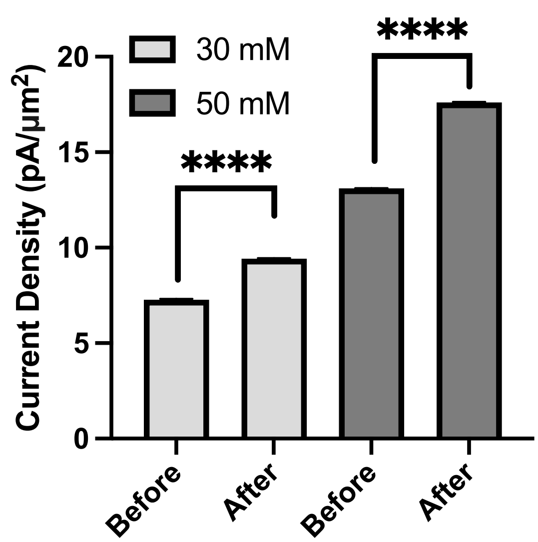

Figure 9. Comparison between current density recorded after 30 mM or 50 mM ACh injection onto 1:18.7 AChE:ChO modified CFMs, separated by before and after implementing proper storage and handling procedures. Error bars are ±1 SEM, n=3-5 electrodes per condition. ****$p<0.0001$

did not have access to one. We found significant increases in current output from both 30 mM and 50 mM ACh injections after handling and storing ACh properly ($p<0.0001$; Figure 8), indicating that the concentration tested in the before condition was likely lower than presumed. This emphasizes the importance of proper storage and confirms that any ACh sample exposed to air over a period of time will likely yield unreliable and unusable data.

Conclusions

ACh is an important molecule to further understand due to its ties with epilepsy as well as learning and memory. We established that a 1:10 ratio of AChE:ChO on a CFMs holds the most promise for *in vivo* detection of ACh due to its highly linear calibration curve, high sensitivity to ACh, and high selectivity. We found that the enzyme-modified CFMs are also highly stable, allowing for continuous *in vivo* monitoring over the course of several hours. Additionally, we were able to record significant hippocampal events *in vivo* following sensory stimulation that were responsive in a spatially and temporally sensitive manner. These modifications therefore hold great promise for elucidating the role of ACh in regulating theta oscillations and, by extension, the role of ACh regulation in epilepsy. In addition to the further testing mentioned throughout the paper, we next hope to test our electrodes in awake as well as freely moving rodents.

Acknowledgements

I would like to acknowledge and thank:

Dr. Yangguang Ou for her unwavering support, guidance, and patience throughout this project and my time in her lab. She has shaped me into an independent researcher and instilled in me a deep appreciation for the scientific process.

Dr. Jeremy Barry for his integral role in the formation of this project and for making the *in vivo* experiments a reality.

Dr. Allison Anacker for her excellent instruction over the past several years, providing me with the learning tools to effectively read and write scientifically.

The OU Lab, especially Margaret O'Neill, Isabella Schapira, and Nikki Vilarini, for their assistance in data collection and troubleshooting, Ryan Hunt for his help in kickstarting the project while rotating through the lab, and Dr. Julia Perdrial for connecting me with the OU Lab.

Senator and Mrs. Leahy, the UVM Office of Fellowships, Opportunities, and Undergraduate Research, the Ronald Suiter Fund, as well as the College of Arts and Sciences for their direct financial support of this project. The Vermont Center for Cardiovascular & Brain Health for the funding of the OU Lab.

References

1. Zack MM, Kobau R. National and State Estimates of the Numbers of Adults and Children with Active Epilepsy - United States, 2015. *MMWR Morb Mortal Wkly Rep*. Aug 11 2017;66(31):821-825. doi:10.15585/mmwr.mm6631a1
2. Hermann BP, Seidenberg M, Dow C, et al. Cognitive prognosis in chronic temporal lobe epilepsy. *Annals of Neurology*. 2006;60(1):80-87. doi:https://doi.org/10.1002/ana.20872
3. Winson J. Loss of Hippocampal Theta Rhythm Results in Spatial Memory Deficit in the Rat. *Science*. 1978;201(4351):160-163. doi:doi:10.1126/science.663646
4. Shuman T, Amendolara B, Golshani P. Theta Rhythmopathy as a Cause of Cognitive Disability in TLE. *Epilepsy Curr*. Mar-Apr 2017;17(2):107-111. doi:10.5698/1535-7511.17.2.107
5. Nuñez A, Buño W. The Theta Rhythm of the Hippocampus: From Neuronal and Circuit Mechanisms to Behavior. Review. *Frontiers in Cellular Neuroscience*. 2021-March-04 2021;15doi:10.3389/fncel.2021.649262
6. MacVicar BA, Tse FW. Local neuronal circuitry underlying cholinergic rhythmical slow activity in CA3 area of rat hippocampal slices. *J Physiol*. Oct 1989;417:197-212. doi:10.1113/jphysiol.1989.sp017797
7. Li S, Topchiy I, Kocsis B. The effect of atropine administered in the medial septum or hippocampus on high- and low-frequency theta rhythms in the hippocampus of urethane anesthetized rats. *Synapse*. Jun 2007;61(6):412-9. doi:10.1002/syn.20388
8. Kramis R, Vanderwolf CH, Bland BH. Two types of hippocampal rhythmical slow activity in both the rabbit and the rat: relations to behavior and effects of atropine, diethyl ether, urethane, and pentobarbital. *Exp Neurol*. Oct 1975;49(1 Pt 1):58-85. doi:10.1016/0014-4886(75)90195-8
9. Gu Z, Yakel JL. Cholinergic Regulation of Hippocampal Theta Rhythm. *Biomedicines*. Mar 23 2022;10(4)doi:10.3390/biomedicines10040745
10. Rodeberg NT, Sandberg SG, Johnson JA, Phillips PE, Wightman RM. Hitchhiker's Guide to Voltammetry: Acute and Chronic Electrodes for in Vivo Fast-Scan Cyclic Voltammetry. *ACS Chem Neurosci*. Feb 15 2017;8(2):221-234. doi:10.1021/acschemneuro.6b00393
11. Hammarlund-Udenaes M. Microdialysis as an Important Technique in Systems Pharmacology—a Historical and Methodological Review. *The AAPS Journal*. 2017/09/01 2017;19(5):1294-1303. doi:10.1208/s12248-017-0108-2
12. Jaquins-Gerstl A, Michael AC. Comparison of the brain penetration injury associated with microdialysis and voltammetry. *J Neurosci Methods*. Oct 15 2009;183(2):127-35. doi:10.1016/j.jneumeth.2009.06.023
13. Zhang H, Lin S-C, Nicolelis MA. Spatiotemporal coupling between hippocampal acetylcholine release and theta oscillations in vivo. *Journal of Neuroscience*. 2010;30(40):13431-13440.
14. Keighron JD, Wigström J, Kurczy ME, Bergman J, Wang Y, Cans A-S. Amperometric Detection of Single Vesicle Acetylcholine Release Events from an Artificial Cell. *ACS Chemical Neuroscience*. 2015/01/21 2015;6(1):181-188. doi:10.1021/cn5002667
15. Navera EN, Suzuki M, Tamiya E, Takeuchi T, Karube I. Nafion-coated carbon fiber for acetylcholine and choline sensors. *Electroanalysis*. 1993;5(1):17-22. doi:https://doi.org/10.1002/elan.1140050105

16. Ou Y, Buchanan AM, Witt CE, Hashemi P. Frontiers in Electrochemical Sensors for Neurotransmitter Detection: Towards Measuring Neurotransmitters as Chemical Diagnostics for Brain Disorders. *Anal Methods*. Jun 6 2019;11(21):2738-2755. doi:10.1039/c9ay00055k
17. Dankoski EC, Wightman RM. Monitoring serotonin signaling on a subsecond time scale. *Front Integr Neurosci*. 2013;7:44. doi:10.3389/fnint.2013.00044
18. Keighron JD, Åkesson S, Cans A-S. Coimmobilization of Acetylcholinesterase and Choline Oxidase on Gold Nanoparticles: Stoichiometry, Activity, and Reaction Efficiency. *Langmuir*. 2014/09/30 2014;30(38):11348-11355. doi:10.1021/la502538h
19. Sanford AL, Morton SW, Whitehouse KL, et al. Voltammetric Detection of Hydrogen Peroxide at Carbon Fiber Microelectrodes. *Analytical Chemistry*. 2010/06/15 2010;82(12):5205-5210. doi:10.1021/ac100536s
20. Hashemi P, Dankoski EC, Petrovic J, Keithley RB, Wightman RM. Voltammetric Detection of 5-Hydroxytryptamine Release in the Rat Brain. *Analytical Chemistry*. 2009/11/15 2009;81(22):9462-9471. doi:10.1021/ac9018846
21. Kloc ML, Daglian JM, Holmes GL, Baram TZ, Barry JM. Recurrent febrile seizures alter intrahippocampal temporal coordination but do not cause spatial learning impairments. *Epilepsia*. 2021;62(12):3117-3130. doi:https://doi.org/10.1111/epi.17082
22. Kloc ML, Chen Y, Daglian JM, Holmes GL, Baram TZ, Barry JM. Spatial learning impairments and discoordination of entorhinal-hippocampal circuit coding following prolonged febrile seizures. *Hippocampus*. Apr 24 2023;doi:10.1002/hipo.23541
23. Bourne Y, Grassi J, Bougis PE, Marchot P. Conformational flexibility of the acetylcholinesterase tetramer suggested by x-ray crystallography. *J Biol Chem*. Oct 22 1999;274(43):30370-6. doi:10.1074/jbc.274.43.30370
24. Quaye O, Lountos GT, Fan F, Orville AM, Gadda G. Role of Glu312 in binding and positioning of the substrate for the hydride transfer reaction in choline oxidase. *Biochemistry*. Jan 8 2008;47(1):243-56. doi:10.1021/bi7017943
25. Descarries L, Gisiger V, Steriade M. Diffuse transmission by acetylcholine in the CNS. *Prog Neurobiol*. Dec 1997;53(5):603-25. doi:10.1016/s0301-0082(97)00050-6
26. Vinson PN, Justice JB, Jr. Effect of neostigmine on concentration and extraction fraction of acetylcholine using quantitative microdialysis. *J Neurosci Methods*. Apr 25 1997;73(1):61-7. doi:10.1016/s0165-0270(96)02213-3
27. Aidoo AY, Ward K. Spatio-temporal concentration of acetylcholine in vertebrate synaptic cleft. *Mathematical and Computer Modelling*. 2006/11/01/ 2006;44(9):952-962. doi:https://doi.org/10.1016/j.mcm.2006.03.003
28. Rice ME. H2O2: a dynamic neuromodulator. *Neuroscientist*. Aug 2011;17(4):389-406. doi:10.1177/1073858411404531
29. Brankack J, Stewart M, Fox SE. Current source density analysis of the hippocampal theta rhythm: associated sustained potentials and candidate synaptic generators. *Brain Res*. Jul 2 1993;615(2):310-27. doi:10.1016/0006-8993(93)90043-m
30. Dickson CT, Trepel C, Bland BH. Extrinsic modulation of theta field activity in the entorhinal cortex of the anesthetized rat. *Hippocampus*. Feb 1994;4(1):37-51. doi:10.1002/hipo.450040106
31. Hanada Y, Hallworth NE, Szgatti TL, Scarlett D, Bland BH. Distribution and analysis of hippocampal theta-related cells in the pontine region of the urethane-anesthetized rat.

Hippocampus. 1999;9(3):288-302. doi:10.1002/(sici)1098-1063(1999)9:3<288::Aid-hipo8>3.0.Co;2-a
32. Hölscher C, Anwyl R, Rowan MJ. Stimulation on the positive phase of hippocampal theta rhythm induces long-term potentiation that can Be depotentiated by stimulation on the negative phase in area CA1 in vivo. *J Neurosci*. Aug 15 1997;17(16):6470-7. doi:10.1523/jneurosci.17-16-06470.1997
33. Klausberger T, Magill PJ, Márton LF, et al. Brain-state- and cell-type-specific firing of hippocampal interneurons in vivo. *Nature*. Feb 20 2003;421(6925):844-8. doi:10.1038/nature01374
34. Klausberger T, Somogyi P. Neuronal diversity and temporal dynamics: the unity of hippocampal circuit operations. *Science*. Jul 4 2008;321(5885):53-7. doi:10.1126/science.1149381
35. Lockmann ALV, Laplagne DA, Leão RN, Tort ABL. A Respiration-Coupled Rhythm in the Rat Hippocampus Independent of Theta and Slow Oscillations. *The Journal of Neuroscience*. 2016;36(19):5338-5352. doi:10.1523/jneurosci.3452-15.2016
36. Vanderwolf CH. Cerebral activity and behavior: control by central cholinergic and serotonergic systems. *Int Rev Neurobiol*. 1988;30:225-340. doi:10.1016/s0074-7742(08)60050-1
37. Quintanilla L, Su Y, Simon JM, et al. Basal forebrain cholinergic circuits orchestrate diverse cell types in the adult dentate gyrus to support neural stem cell function and spatial memory. *bioRxiv*. 2022:2022.05.25.493227. doi:10.1101/2022.05.25.493227
38. Ogando MB, Pedroncini O, Federman N, et al. Cholinergic modulation of dentate gyrus processing through dynamic reconfiguration of inhibitory circuits. *Cell Reports*. 2021/08/24/ 2021;36(8):109572. doi:https://doi.org/10.1016/j.celrep.2021.109572
39. Dannenberg H. *Direct and indirect cholinergic septo-hippocampal pathways cooperate to structure spiking activity in the hippocampus*. Bonn, Rheinische Friedrich-Wilhelms-Universität Bonn, Diss., 2015; 2015.